Preparation and Physical Characterization of Pyrene and Pyrrolo[3,4-c]pyrrole-1,4-dione-Based Copolymers

Bakhet A. Alqurashy*[a]

Two narrow band-gap copolymers consisting of 2,7-bis(5-(trimethylstannyl)thiophen-2-yl)-4,5,9,10-tetrakis(2-ethylhexy-loxy)-pyrene (M1) as an electron-rich unit and diketopyrrolopyr-role (DPP) as an electron-deficient unit have been synthesized and characterized for polymer solar cells. The two polymers were prepared by Stille coupling reactions. Two solubilizing alkyl chains (ethylhexyl and octlydodecyl) were attached to the DPP unit in order to evaluate their impact upon the optical and electrochemical characteristics of the two polymers. Poly [4,5,9,10-tetrakis[(2-ethylhexyl)oxy]pyrene-alt-3,6-bis(thiophen-2-yl)-2,5- bis(2-octyldodecyl)pyrrole[3,4-c]pyrrole- 1,4(2H,5H)-di-one] (PP$_{EH}$DT-DPP$_{ODo}$) and poly[4,5,9,10-tetrakis((2-ethylhexyl) oxy)pyren-alt-3,6-bis(thiophen-2-yl)-2,5-bis(2-ethylhexyl)pyrrole [3,4-c]pyrrole-1,4(2H,5H)-dione] (PP$_{EH}$DT-DPP$_{EH}$) exhibited high thermal stability with decomposition temperatures over 300 °C.

Optical properties showed that PP$_{EH}$DT-DPP$_{ODo}$ and PP$_{EH}$DT-DPP$_{EH}$ have optical band gaps of around 1.40 eV. It is believed that both polymers adopt high planar structures in the thin film, leading to more electronic conjugation along the back-bone of the conjugated polymers. Powder X-ray diffraction revealed that PP$_{EH}$DT-DPP$_{ODo}$ and PP$_{EH}$DT-DPP$_{EH}$ seem to have an amorphous nature. The HOMO energy levels of the two polymers are clearly affected by changing alkyl chains. The HOMO levels of PP$_{EH}$DT-DPP$_{ODo}$ and PP$_{EH}$DT-DPP$_{EH}$ were found to be at −5.27 and −5.38 eV, respectively. PP$_{EH}$DT-DPP$_{ODo}$ showed a HOMO energy level approximately 0.11 eV shallower than that of PP$_{EH}$DT-DPP$_{EH}$, which is probably a consequence of attaching a larger alkyl chain to the DPP moiety reducing its electron accepting ability.

1. Introduction

Over the last decades, organic solar cell (OSC) materials consisting of conjugated polymers as an electron donor and fullerene derivatives as an electron acceptor have been considered as one of the promising sustainable energy sources due to several features including, flexibility, solution process-ability, ease of manufacturing, they are affordable and recyclable materials.[1–3] Consequently, conjugated polymers-fullerene derivatives based bulk heterojunction (BHJ) devices have led to considerable development in the OSC performance rising the power conversion efficiency of organic solar cell BHJ devices in excess of 10%.[4,5] This achievement is assigned to the significant improvement of new conjugated polymers which display improved hole transporting properties, higher spectral sensitivity and adjusted HOMO/LUMO energy levels that is compatible with those of fullerene derivatives.[1,6]

In the last few years, a considerable amount of efforts and research has been placed in the synthesizing of novel conjugated polymers. While, the fullerene derivatives are still the common acceptors applied in BHJ devices until now. This is mainly due to their remarkable electron-transporting and -accepting properties. The poor absorption in the near-IR and visible region is considered to be the substantial problem of fullerene derivatives.[7,8]

The original buckminsterfullerene (C$_{60}$) displayed poor solubility in common organic solvents. Consequently, the need of inserting solubilizing group to the original C$_{60}$ was adopted in order to enhance the solubility.[9,10] [6,6]-phenyl-C61-butyric acid methyl ester (PC$_{61}$BM) was approached and it has many advantages when compared with C$_{60}$, for example good solubility, outstanding electron-affinity as well as -mobility.[11,12] However, PC$_{61}$BM possess low LUMO energy level which limit the short circuit current (J$_{SC}$) of the PV device and also restrict the required energy level for the p-type materials (the conjugated polymer) to accomplish high open circuit voltage (V$_{OC}$) value.[7] Adjusting the LUMO levels of the n-type materials (fullerene derivatives) relative to the LUMO levels of the p-type materials is the major challenge; since this technique would lead to reduction in the thermalization losses.[7,13] PC$_{71}$BM exhibited a lower degree of symmetric when compared with PC$_{61}$BM, and as a result PC$_{71}$BM would display larger optical transitions. This feature would shift the absorption bands towards the visible region resulting in high J$_{SC}$ values.[7,12]

Pyrrolo[3,4-c]pyrrole-1,4-dione (or Diketopyrrolopyrrole (DPP)) was first synthesized in 1974 by Farnum et al. In 2008, Janssen and Nguyen applied DPP-polymers and –small mole-cules, respectively, for the first time in the field of organic photovoltaic devices. Ever since, DPP has been intensively used as an electron-accepting moiety in organic solar cell.[5] The DPP-polymers moiety generally consists of two solubilizing side chains attached to the imide groups, a central π-conjugated part and two flanked neighboring aromatic units. The solubility

[a] Dr. B. A. Alqurashy
Department of Basic Science and Technologies
Community Faculty, Taibah University
30002, Al-Madina Al-Mounawara, Saudi Arabia
E-mail: Bqourasy@taibahu.edu.sa

Table 1. Characteristics of PP$_{EH}$DT-DPP$_{ODo}$ and PP$_{EH}$DT-DPP$_{EH}$.

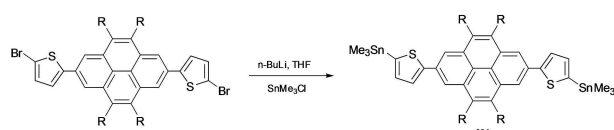| Polymer	M_n[c] [Da]	M_w[c] [Da]	PDI	λ_{max} [nm] Solution	Film	$E_{g\,opt}$[d] [eV]	HOMO[e] [eV]	LUMO[e] [eV]	E_g elec[f] [eV]
PP$_{EH}$DT-DPP$_{ODo}$[a]	5500	11800	2.14	631	695	1.42	−5.27	−3.57	1.70
PP$_{EH}$DT-DPP$_{EH}$[b]	6900	15300	2.20	657	695	1.39	−5.38	−3.57	1.81

[a] Measurements conducted on the hexane fraction of the polymers. [b] Measurements conducted on the toluene fraction of the polymers. [c] GPC conducted in 1,2,4-trichlorobenzene at 140 °C. [d] Eg determined from the onset of the absorption band in thin film. [e] HOMO and LUMO levels determined from the cyclic voltammetry. [f] Electrochemical band gap.

of DPP-based co-polymers can be significantly tuned by alternations in the polymer backbone.[14] Furthermore, the electron accepting nature of DPP means that the DPP moiety can be co-polymerized with different electron donor units. The DPP unit has a planar structure resulting in a high π-π interaction along the conjugated backbone which give rise to a high intramolecular charge transfer (ICT). Hence, DPP-based polymers exhibited narrow band gaps about 1.3 eV, owing to their wide absorptions spectra between 600 and 900 nm.[11,15] Devices fabricated from polymers based on DPP displayed high J$_{SC}$ which is probably owing to attaching electron donating thienyl units. However, these devices have low Voc as a result of raising of the HOMO energy level.[11,15] Devices fabricated from DPP-based polymers as an electron donor showed a power conversion efficiency higher than 9%.[5,16,17]

In this work, two copolymers consisting of pyrene as the electron rich moiety and the high planner DPP as the electron deficient moiety, (**PP$_{EH}$DT-DPP$_{ODo}$** and **PP$_{EH}$DT-DPP$_{EH}$**), were synthesized and characterized. Here, DPP was introduced to reduce the band-gap of pyrene-based copolymers. Furthermore, to further improve the optical and electrochemical properties of the polymers, two types of DPP derivatives were used. The two polymers were synthesized by Stille coupling. Cyclic voltammograms (CV) and UV-vis spectroscopy were analyzed to investigate the HOMO/LUMO energy levels and optical properties of the two polymers. Both polymers displayed narrow band-gaps of around 1.40 eV, and slightly deep HOMO levels

produced **PP$_{EH}$DT-DPP$_{ODo}$** and **PP$_{EH}$DT-DPP$_{EH}$**, respectively (Scheme 2). Both polymers are soluble in common organic solvent. The weight-average molecular weights (M$_w$) of **PP$_{EH}$DT-DPP$_{ODo}$** and **PP$_{EH}$DT-DPP$_{EH}$** are 11800–15300 Da, respectively, and the results are summarized in Table 1, as determined by gel permission chromatography (GPC). **PP$_{EH}$DT-DPP$_{ODo}$** displayed lower molecular weights relative to **PP$_{EH}$DT-DPP$_{EH}$**. It is believed that the low molecular weights of **PP$_{EH}$DT-DPP$_{ODo}$** is a result of steric hindrance between ethylhexyloxy substituents on **M1** and octyldodecyl substituents on **M2**. It is also possible that these interactions decrease the planarity of the conjugated polymer backbone.

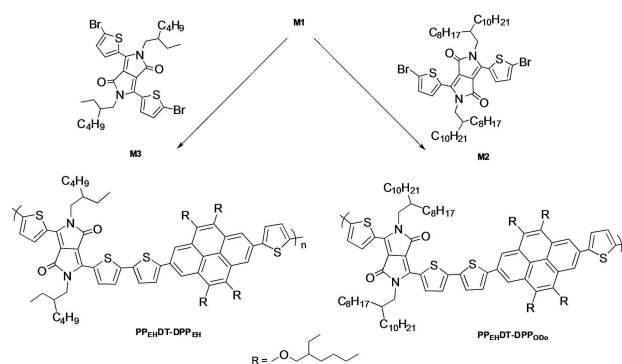**Scheme 2.** Synthesis of PP$_{EH}$DT-DPP$_{ODo}$ and PP$_{EH}$DT-DPP$_{EH}$.

2. Results and Discussion

For the synthesis of the two polymers, M1 was prepared through functionalization of 2,7-Bis(5-bromo-thien-2-yl)-4,5,9,10-tetrakis(2-ethylhexyloxy)-pyrene (1) by trimethyltin chloride in the presence of n-butyllithium (Scheme 1).[18,19] M2 and M3 were prepared according to literature procedures.[20–22] Stille coupling reaction of **M1** with **M2** and also with **M3**,

Scheme 1. Synthetic route towards monomers M1.

2.1. UV/Vis Absorption Spectroscopy

The UV-vis absorption spectra of **PP$_{EH}$DT-DPP$_{ODo}$** and **PP$_{EH}$DT-DPP$_{EH}$** were recorded in thin film (Figure 1a) and chloroform solution (Figure 1b), and the data are outlined in Table 1. The tow polymers showed a strong absorption at shorter wavelengths which are attributed to π-π* transitions. In solution, **PP$_{EH}$DT-DPP$_{ODo}$** and **PP$_{EH}$DT-DPP$_{EH}$** showed a main absorption band at 614 and 657 nm, respectively, as a result of the intramolecular charge transfer (ICT) from the electron donor pyrene units and thiophene rings to the electron acceptor DPP units. In solid state, the absorption bands of **PP$_{EH}$DT-DPP$_{ODo}$** and **PP$_{EH}$DT-DPP$_{EH}$** were red-shifted to 695 nm. These redshifts can be ascribed to a more ordered structure and more planar conjugated backbone in the solid state.
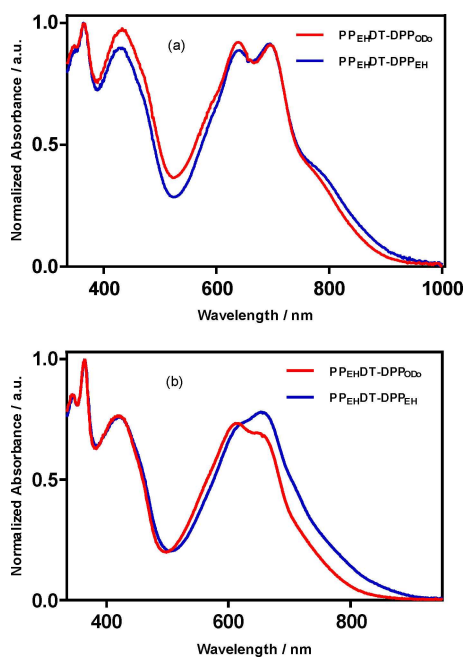
Figure 1. UV/Vis absorption spectra of **PP$_{EH}$DT-DPP$_{ODo}$** and **PP$_{EH}$DT-DPP$_{EH}$** in: a) thin films and b) chloroform solutions.

Figure 2. Cyclic voltammograms of thin films of **PP$_{EH}$DT-DPP$_{ODo}$** and **PP$_{EH}$DT-DPP$_{EH}$** on platinum disc electrodes (area 0.031 cm^2) at a scan rate of 100 mV s^{-1} in acetonitrile / tetrabutyl ammonium perchlorate (0.1 mol dm^{-3}).

Additionally, the two polymers exhibited an additional peak at lower wavelength between 390 and 465 nm in both solution and solid state. However, the peak intensity of **PP$_{EH}$DT-DPP$_{ODo}$** and **PP$_{EH}$DT-DPP$_{EH}$** is more pronounced in the solid state. This is a result of a higher planar conformations in the solid state resulting in a higher electronic conjugation along the polymer conjugated backbone.

The optical band gaps of **PP$_{EH}$DT-DPP$_{ODo}$** and **PP$_{EH}$DT-DPP$_{EH}$** were calculated from their onsets of absorption in films and found to be 1.42 and 1.39 eV, respectively. **PP$_{EH}$DT-DPP$_{EH}$** displayed a narrower optical band gap compared to **PP$_{EH}$DT-DPP$_{ODo}$**. This can be ascribed to the solubilizing chain attached to the DPP acceptor moieties on the respective polymers.

Generally, adding solubilizing alkyl chains to the polymers backbones is a crucial technique to adjust the peaks absorptions intensities as well as to achieve the desired sunlight absorption. This method is important for preparing new polymers that are applicable for use in organic solar cells devices.

2.2. Cyclic Voltammetry

To determine the electrochemical properties of **PP$_{EH}$DT-DPP$_{ODo}$** and **PP$_{EH}$DT-DPP$_{EH}$**, cyclic voltammetry (CV) was applied to evaluate the HOMO/ LUMO energy levels, and the data are outlined in Table 1. As shown in Figure 2, the HOMO/LUMO energy levels of **PP$_{EH}$DT-DPP$_{ODo}$** and **PP$_{EH}$DT-DPP$_{EH}$** were found to be at −5.27/−3.57 and −5.38/−3.57 eV, respectively. The **PP$_{EH}$DT-DPP$_{EH}$** polymer showed a HOMO energy level ~0.11 eV deeper than that of the **PP$_{EH}$DT-DPP$_{ODo}$** polymer.

The shallower HOMO level of **PP$_{EH}$DT-DPP$_{ODo}$** is probably a consequence of attaching a larger alkyl chain (octyldodecyl) to the **DPP** moiety reducing its electron accepting ability which in turn reduces the ICT along the polymer chain. The results display that alternation of different alkyl chains on the DPP moiety does not show any change on the LUMO energy levels of the two polymers; but it shows a clear influence on the HOMO energy levels.

When comparing the pyrene-DPP based copolymers synthesized in this contribution with pyrene-TPD based copolymers, **PP$_{EH}$DT-TPD$_{O}$** and **PP$_{EH}$DT-TPD$_{HP}$**, prepared by Alqurashy *et al*,[18] it is clear that the TPD moiety significantly determines the HOMO/LUMO energy levels. The HOMO levels of **PP$_{EH}$DT-TPD$_{O}$** and **PP$_{EH}$DT-TPD$_{HP}$** were estimated to be −5.57 and −5.55 eV, respectively, which is largely deeper than those of the **PP$_{EH}$DT-DPP$_{ODo}$** and **PP$_{EH}$DT-DPP$_{EH}$** proposing that the existence of the strongly electron-accepting TPD moiety can lower the HOMO level. In addition, **PP$_{EH}$DT-TPD$_{O}$** and **PP$_{EH}$DT-TPD$_{HP}$** displayed LUMO levels slightly higher in energy −3.59 and −3.54 eV, respectively, resulting in a higher electrochemical band gap, 1.98 and 2.01, respectively, compared to **PP$_{EH}$DT-DPP$_{ODo}$** and **PP$_{EH}$DT-DPP$_{EH}$** polymers. These data reveal that the presence of the TPD moiety in the conjugated polymer backbone largely affect the HOMO/LUMO energy levels compared to DPP moiety. It is believed that the use of TPD moiety in the conjugated polymer backbone seems to lower the HOMO energy level, which is beneficial for obtaining high V$_{oc}$ values in OPV devices. However, the alternating polymers comprising DPP moiety would absorb sunlight in the UV-vis-NIR region, and accordingly enhance the Jsc.

The electrochemical band-gap calculated to be 1.70 and 1.81 eV for **PP$_{EH}$DT-DPP$_{ODo}$** and **PP$_{EH}$DT-DPP$_{EH}$**, respectively, which is higher than the optical band gap owing to the exciton binding energy of the conjugated polymers.

2.3. Thermal Properties

The thermal stability of the **PP$_{EH}$DT-DPP$_{ODo}$** and **PP$_{EH}$DT-DPP$_{EH}$** was analyzed by thermogravimetric analysis (TGA), as illustrated in Figure 3. The TGA of the two polymers revealed that the decomposition temperatures (5% weight loss) were 340 °C for both **PP$_{EH}$DT-DPP$_{ODo}$** and **PP$_{EH}$DT-DPP$_{EH}$**. The two polymers
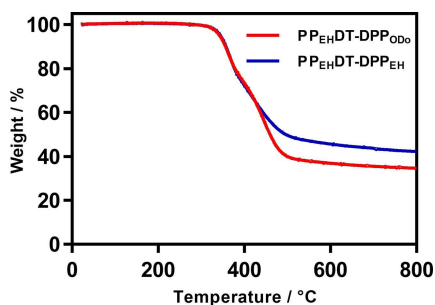
Figure 3. TGA curves of PP$_{EH}$DT-DPP$_{ODo}$ and PP$_{EH}$DT-DPP$_{EH}$.

showed good thermal stability, which is beneficial for use in polymer solar cells.

2.4. Powder X-ray Diffraction (PXRD)

The molecular organization of the two pyrene-DPP based copolymers was investigated in the solid state using powder X-ray diffraction (PXRD) (Figure 4). PP$_{EH}$DT-DPP$_{EH}$ showed a poorly resolved peak at $2\theta = 3.75°$ corresponding to a d-spacing of 23.54 Å, which is characteristic for inter-chain distances detached by the alkyl or alkoxy side-chains. Also, PP$_{EH}$DT-DPP$_{EH}$ exhibited a broad diffuse peak at $2\theta = 21.6°$, which correspond to a π-π stacking distance between conjugated polymer backbones corresponding to a d-spacing of 4.11 Å. PP$_{EH}$DT-DPP$_{ODo}$ displayed a poorly single broad diffuse peak at wide angle region at $2\theta = 21.9°$, which correspond to a d-spacing of 4.05 Å. The absence of peaks in the small angle region indicates that PP$_{EH}$DT-DPP$_{ODo}$ does not have any arranged structure; which means that the polymer seems to display an amorphous structure in the solid state.

3. Conclusions

Two new donor-acceptor narrow band gap conjugated polymers using pyrene as an electron rich unit and DPP as an electron acceptor units, PP$_{EH}$DT-DPP$_{ODo}$ and PP$_{EH}$DT-DPP$_{EH}$, were designed and synthesized for polymer solar cell applications. The two polymers were characterized by using ^{1}H NMR, TGA, UV-vis absorption, cyclic voltammetry and powder X-ray
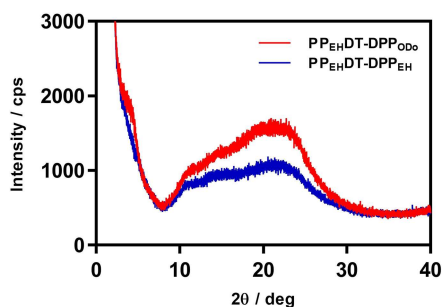

Figure 4. PXRD patterns of PP$_{EH}$DT-DPP$_{ODo}$ and PP$_{EH}$DT-DPP$_{EH}$.

diffraction. Two different alkyl chains (ethylhexyl and octlydo-decyl) were attached to the DPP units along polymer backbones to assess their impact on the photophysical and electronic characteristic of the resulting polymers. Characterization show that PP$_{EH}$DT-DPP$_{ODo}$ and PP$_{EH}$DT-DPP$_{EH}$ have narrow optical bandgaps of 1.42 and 1.39 eV, relatively deep HOMO energy levels of -5.27 and -5.38 eV. PP$_{EH}$DT-DPP$_{EH}$ displayed higher molecular weight and relatively narrower optical band gaps relative to PP$_{EH}$DT-DPP$_{ODo}$. It is thought the attachment of shorter alkyl chains are responsible for this. PXRD analysis suggested that the polymer with shorter alkyl chains, PP$_{EH}$DT-DPP$_{EH}$, showed smaller π-π stacking distances compared to the polymer with larger alkyl chains, PP$_{EH}$DT-DPP$_{ODo}$.

Experimental Section

Materials

All chemicals and materials were obtained from commercial sources and used as received, unless otherwise stated. Toluene was dried and distilled over sodium metal under an inert argon atmosphere. Acetonitrile was dried and distilled over phosphorous pentoxide and stored under an inert atmosphere with molecular sieves (3 Å). For supporting information regarding materials, measurements and instrument see reference 18 and 23.

Preparation of Monomers and Polymers

2,7-Bis(5-(trimethylstannyl)thiophen-2-yl)-4,5,9,10-tetrakis (2-ethylhexyloxy)-pyrene (M1)

Under an inert atmosphere, 2,7-Bis(5-bromo-thien-2-yl)-4,5,9,10-tetrakis(2-ethylhexyloxy)-pyrene (**1**) (0.41 g, 0.40 mmol) was dissolved in 20 mL of anhydrous tetrahydrofuran. The solution was cooled down to $-78°C$ and then n-BuLi (2.5 M in hexanes, 0.48 ml, 1.2 mmol) was added dropwise. The reaction mixture was left to stir for 3 hours at $-78°C$. Trimethyltin chloride (0.24 g, 1.2 mmol) was dissolved in 3 mL of anhydrous THF which was then added dropwise. Then, the solution was left to warm to room temperature and left to stir overnight. The reaction mixture was poured onto brine and extracted with diethyl ether (4 x 100 mL). The organic phase was washed with water (4×80 mL) and dried over MgSO$_4$. The solvent was removed *in vacuo* to obtain the target product as a yellow solid (0.29 g, 0.24 mmol, 60.1%). ^{1}H-NMR (400 MHz, CDCl$_3$) (δ_H/ppm): 8.70 (s, 4H), 7.75 (d, $J = 3.08$ Hz, 2H), 7.30 (d, $J = 3.79$ Hz, 2H), 4.28 (d, $J = 5.92$ Hz, 8H), 2.04–1.93 (m, 4H), 1.85-1.37 (m, 32H), 1.08 (t, $J = 7.56$ Hz, 12H), 0.96 (t, $J = 7.07$ Hz, 12H), 0.47 (s, 18H). ^{13}C NMR (400 MHz, CDCl$_3$) (δ_C/ppm): 151.36, 144.68, 138.30, 136.47, 132.07, 129.12, 124.74, 120.15, 116.28, 40.93, 30.86, 29.45, 23.96, 23.30, 14.23, 11.38, -8.22. GC-MS mass calcd. for C$_{62}$H$_{94}$O$_4$S$_2$Sn$_2$ 1206.46; Found 1206.59.

Poly[4,5,9,10-tetrakis[(2-ethylhexyl)oxy]pyrene-alt-3,6-bis (thiophen-2-yl)-2,5- bis(2-octyldodecyl)pyrrole[3,4-c]pyrrole-1,4(2H,5H)-dione] (PP$_{EH}$DT-DPP$_{ODo}$):

M1 (0.165 g, 0.160 mmol) and **M2** (0.162 g, 0.160 mmol) were first dissolved in 5 mL of anhydrous toluene and the mixture was degassed using argon followed by the addition of Pd(OAc)$_2$ (2.00 mg, 11 μmol) and tri(*o*-toly)phosphine (7.00 mg, 23 μmol). The solution was heated to 100°C and lift to stir for over 50 hours.

Then, the reaction mixture was cooled to room temperature and the organic solution was concentrated *in vacuo* to ~40 mL and precipitated in methanol (200 mL). The resulting solid was collected *via* filtration and washed by using Soxhlet extraction with methanol, acetone and hexane. The hexane fraction was filtered, and the polymer was obtained as a dark green solid (150 mg, 0.090 mmol, 55.8%). GPC hexane fraction: $M_n = 5,500$ Da; $M_w = 11,800$ Da; PDI $= 2.14$. ^{1}H-NMR (500 MHz, $C_2D_2Cl_4$, 100°C): (δ_H/ppm) 8.78–8.66 (br, 6H), 7.60 (d, 2H), 7.48–7.34 (br, 4H), 4.3 (d, 8H), 4.14–3.95 (br, 4H), 2.11–1.97 (br, 4H), 1.90–1.20 (br, 90H), 1.14 (br.t, 12H), 0.99 (br.t, 12H), 0.80 (br.m, 12H). Elem. Anal. Calculated for $C_{106}H_{154}N_2O_6S_4$: C, 75.75; H, 9.24; N, 1.67; S, 7.63. Found: C, 74.98; H, 9.23; N, 1.14; S, 7.09.

Poly[4,5,9,10-tetrakis((2-ethylhexyl)oxy)pyren-alt-3,6-bis(thiophen-2-yl)-2,5-bis(2-ethylhexyl)pyrrole[3,4-c]pyrrole-1,4(2H,5H)-dione] (PP*EH*DT-DPP*EH*):

PP*EH*DT-DPP*EH* was synthesized according to the polymerization method outlined for **PP*EH*DT-DPP*ODo*,** using a mixture of **M1** (0.169 g, 0.140 mmol), **M3** (0.095 g, 0.140 mmol), Pd(OAc)$_2$ (2.00 mg, 11 μmol) and tri(*o*-toly)phosphine (7.00 mg, 23 μmol) in toluene (5 mL). However, the main fraction of the polymer was obtained in toluene. The polymer was obtained as a dark green solid (136 mg, 0.097 mmol, 69.38%). GPC toluene fraction: $M_n = 6,900$ Da; $M_w = 15,300$ Da; PDI $= 2.20$. ^{1}H-NMR (500 MHz, $C_2D_2Cl_4$, 100°C): (δ_H/ppm) 8.78–8.66 (br, 6H), 7.60 (d, 2H), 7.50–7.34 (br, 4H), 4.34 (d, 8H), 4.14–3.95 (br, 4H), 2.11–1.97 (br, 4H), 1.90–1.20 (br, 50H), 1.14 (br.t, 12H), 1.00 (br.t, 12H), 0.80 (br.m, 12H).Elem. Anal. Calculated for $C_{86}H_{114}N_2O_6S_4$: C, 73.77; H, 8.21; N, 2.00; S 9.16. Found: C, 73.68; H, 8.06; N, 1.89; S, 8.88.

Conflict of Interest

The authors declare no conflict of interest.

[1] J. W. Jung, F. Liu, T. P. Russell, W. H. Jo, *Adv. Energy Mater.* **2015**, *5*, 1500065.
[2] S. W. Chang, T. Muto, T. Kondo, M. J. Liao, M. Horie, *Polym. J.* **2017**, *49*, 113–122.
[3] C. Liu, C. Yi, K. Wang, Y. Yang, R. S. Bhatta, M. Tsige, S. Xiao, X. Gong, *ACS Appl. Mater. Interfaces* **2015**, *7*, 4928–4935.
[4] F. Liu, Z. Zhou, C. Zhang, T. Vergote, H. Fan, F. Liu, X. Zhu, *J. Am. Chem. Soc.* **2016**, *138*, 15523–15526.
[5] A. Tang, C. Zhan, J. Yao, E. Zhou, *Adv. Mater.* **2017**, *29*, 1600013.
[6] Y. Lin, J. Wang, Z. G. Zhang, H. Bai, Y. Li, D. Zhu, X. Zhan, *Adv. Mater.* **2015**, *27*, 1170–1174.
[7] C. Soc, K. A. Mazzio, C. K. Luscombe, *Chem. Soc. Rev.* **2014**, *44*, 78–90.
[8] Y. Cheng, S. Yang, C. Hsu, *Chem. Rev.* **2009**, 109, 5868–5923.
[9] G. Yu, J. Gao, J. C. Hummelen, F. Wudl, A. J. Heeger, *Science* **1995**, 270, 1789–1791.
[10] W. Cao, J. Xue, *Energy Environ. Sci.* **2014**, 7, 2123–2144.
[11] H. Zhou, L. Yang, W. You, *Macromolecules* **2012**, *45*, 607–632.
[12] Y. He, H. Chen, J. Hou, Y. Li, *J. Am. Chem. Soc.* **2010**, 132, 1377–1382.
[13] B. C. J. Brabec, S. Gowrisanker, J. J. M. Halls, D. Laird, S. Jia, S. P. Williams, *Adv. Mater.* **2010**, *22*, 3839–3856.
[14] Y. Ji, C. Xiao, Q. Wang, J. Zhang, C. Li, Y. Wu, Z. Wei, X. Zhan, W. Hu, Z. Wang, *Adv. Mater.* **2016**, *28*, 943–950.
[15] H. Guo, C. Weng, G. Wang, B. Zhao, S. Tan, *Dyes Pigm.* **2016**, *133*, 16–24.
[16] J. W. Jung, W. H. Jo, *Polym. Chem.* **2015**, *6*, 4013–4019.
[17] H. Choi, S. J. Ko, T. Kim, P. O. Morin, B. Walker, B. H. Lee, M. Leclerc, J. Y. Kim, A. J. Heeger, *Adv. Mater.* **2015**, *27*, 3318–3324.
[18] B. A. Alqurashy, A. Iraqi, Y. Zhang, D. G. Lidzey, *Eur. Polym. J.* **2016**, *85*, 225–235.
[19] J. Y. Li, C. Y. Chen, C. P. Lee, S. C. Chen, T. H. Lin, H. H. Tsai, K. C. Ho, C. G. Wu, *Org. Lett.* **2010**, *12*, 5454–5457.
[20] R. Ferro, A. Besostri, A. Olivieri, E. Stellini, *Eur. J. Paediatr. Dent.* **2016**, *17*, 36–42.
[21] L. Huo, J. Hou, H. Y. Chen, S. Zhang, Y. Jiang, T. L. Chen, Y. Yang, *Macromolecules* **2009**, *42*, 6564–6571.
[22] P. Sonar, S. P. Singh, E. L. Williams, Y. Li, M. S. Soh, A. Dodabalapur, *J. Mater. Chem.* **2012**, *22*, 4425–4435.
[23] B. A. Alqurashy, L. Cartwright, A. Iraqi, Y. Zhang, D. G. Lidzey, *Polym. Adv. Technol.* **2017**, *28*, 193–200.